

# Extended and symmetric loss of stability for canards in planar fast-slow maps

Maximilian Engel\* and Hildeberto Jardón-Kojakhmetov†

October 4, 2022

## Abstract

We study fast-slow maps obtained by discretisation of planar fast-slow systems in continuous time. We focus on describing the so-called delayed loss of stability induced by the slow passage through a singularity in fast-slow systems. This delayed loss of stability can be related to the presence of canard solutions. Here we consider three types of singularities: transcritical, pitchfork, and fold. First, we show that under an explicit Runge-Kutta discretisation the delayed loss of stability, due to slow passage through a transcritical or a pitchfork singularity, can be arbitrarily long. In contrast, we also show that under a Kahan-Hirota-Kimura discretisation scheme, the delayed loss of stability related to all three singularities is completely symmetric in the linearised approximation, in perfect accordance with the continuous time setting.

## 1 Introduction

Consider a system of singularly perturbed ordinary differential equations (ODEs) in *fast* time scale

$$\begin{aligned} \frac{dx}{dt} &= x' = f(x, y, \varepsilon), \\ \frac{dy}{dt} &= y' = \varepsilon g(x, y, \varepsilon), \quad x \in \mathbb{R}^m, \quad y \in \mathbb{R}^n, \quad 0 < \varepsilon \ll 1, \end{aligned} \tag{1.1}$$

with *critical manifold*

$$\mathcal{S}_0 = \{(x, y) \in \mathbb{R}^{m+n} : f(x, y, 0) = 0\}. \tag{1.2}$$

The set  $\mathcal{S}_0$  is called *normally hyperbolic* if the matrix  $D_x f(p) \in \mathbb{R}^{m \times m}$  for all  $p \in \mathcal{S}_0$  has no spectrum on the imaginary axis. For a normally hyperbolic and compact  $\mathcal{S}_0$ , *Fenichel Theory* [13, 19, 22, 29] implies that for  $\varepsilon$  sufficiently small, there is a locally invariant *slow manifold*  $\mathcal{S}_\varepsilon$  behaving like a regular perturbation of  $\mathcal{S}_0$ . On the other hand, *loss of normal hyperbolicity*, which occurs whenever  $D_x f(p)$  has at least one eigenvalue on the imaginary axis, is known to be responsible for many complicated dynamic effects, such as relaxation oscillations and mixed mode oscillations [8, 22], that are difficult to analyse rigorously. In this paper we will focus on one of such features found

\*Technische Universität München, Forschungseinheit Dynamics, Zentrum Mathematik, M8, Boltzmannstraße 3, 85748 Garching bei München. (maximilian.engel@tum.de)

†Technische Universität München, Forschungseinheit Dynamics, Zentrum Mathematik, M8, Boltzmannstraße 3, 85748 Garching bei München. (h.jardon.kojakhmetov@tum.de)

when normal hyperbolicity is lost, namely *canards*. In particular, we shall study planar fast-slow systems with a *canard point* at the origin, past whom trajectories connect an attracting branch of the slow manifold with a repelling one, also described as *canard solution* [2, 10, 21]. For continuous time fast-slow systems, these canard solutions allow us to explain why one observes a delay in the onset of instabilities when trajectories slowly cross a singularity [15, 24, 25, 26].

In this paper we focus on (discretised) planar fast-slow systems with canard points associated to three singularities: the transcritical, the pitchfork, and the fold. One important motivation to consider fast-slow systems with the aforementioned singularities is that they are common in models used in the applied sciences, thus organising the behaviour of the corresponding dynamics and playing a crucial role for numerical simulations. For example, transcritical singularities may appear in epidemiological and other population dynamic models [4] and seem to be a generic mechanism for stability loss in some network models [17]; pitchfork bifurcations can be found e.g. in decision making dynamics [14] or biochemical oscillators [28], while the fold singularity is frequently encountered in neuron models [3, 7, 23].

Based on observations in [11] and [1], we consider time discretisations of equation (1.1) and investigate the linearised behaviour along such canard solutions. For example, the canonical form of the transcritical singularity in a fast-slow system reads (up to leading order)

$$\begin{aligned}x' &= x^2 - y^2 + \varepsilon \\y' &= \varepsilon.\end{aligned}\tag{1.3}$$

Its Euler discretisation induces the map  $P : \mathbb{R}^2 \rightarrow \mathbb{R}^2$  given by

$$P(x, y) = (x + h(x^2 - y^2) + h\varepsilon, y + h\varepsilon),\tag{1.4}$$

Analogously to the time-continuous case, the set  $\{x^2 = y^2\}$  is invariant under the iteration of  $P$ . In particular, the orbit

$$\gamma(n) = (x_n, y_n) = (x_0 + nh\varepsilon, x_0 + nh\varepsilon), \quad n \in \mathbb{N},\tag{1.5}$$

corresponds to the “discrete-time maximal canard” in [11]. As we prove below, one now observes that trajectories that start close to the attracting part of such a canard, stay close to the repelling part of the canard for very long times; something one cannot observe in the time-continuous case.

In the case of a pitchfork canonical form

$$\begin{aligned}x' &= x(y - x^2), \\y' &= \varepsilon,\end{aligned}$$

the set  $\{x = 0\}$  is invariant, and the Euler discretisation map (2.48) has the canard trajectory

$$\gamma(n) = (0, y_0 + nh\varepsilon), \quad n \in \mathbb{N}.$$

We observe the same extended delay effect along the canard as in the transcritical case (cf. [1]), as we will make precise in Section 2.2.

Generally, for explicit Runge-Kutta methods, the same effects appear. These delay times of the onset of instability can in fact grow arbitrarily large as we will prove in Section 2.1 by investigating contraction and expansion along the linearisation of the canard. The main result concerning arbitrarily long delay of bifurcations for transcritical and pitchfork singularities can be formulated in the following Theorem, which is sketched in Figure 1.

**Theorem 1.1** (Delay for explicit RK schemes). *Let equation (1.1) be the canonical form of a fast-slow system with transcritical or pitchfork singularity, with parameters such that there is a canard solution, and let  $P$  be the map obtained by an explicit Runge-Kutta discretisation of equation (1.1) with discrete-time maximal canard  $\gamma$ . Denoting by  $x_0 = -\rho < 0$  the initial  $x$ -coordinate, we have the following for the transcritical canard (and analogously for the  $y$ -coordinate in the pitchfork case):*

1. *if  $x^*$  denotes the  $x$ -coordinate where the contraction/expansion rate around  $\gamma$  is compensated, i.e. where trajectories, starting close to  $\gamma$  at  $x_0 = -\rho$ , leave the vicinity of  $\gamma$ , then there exist values  $(\rho^*, h^*, \varepsilon^*)$  such that*

$$\lim_{(\rho, h, \varepsilon) \rightarrow (\rho^*, h^*, \varepsilon^*)} x^* \rightarrow \infty. \quad (1.6)$$

2. *we, moreover, obtain a particular lower bound  $K^*$  for the number of iterations corresponding with  $x^*$ , expressed by the Lambert  $W$  function.*

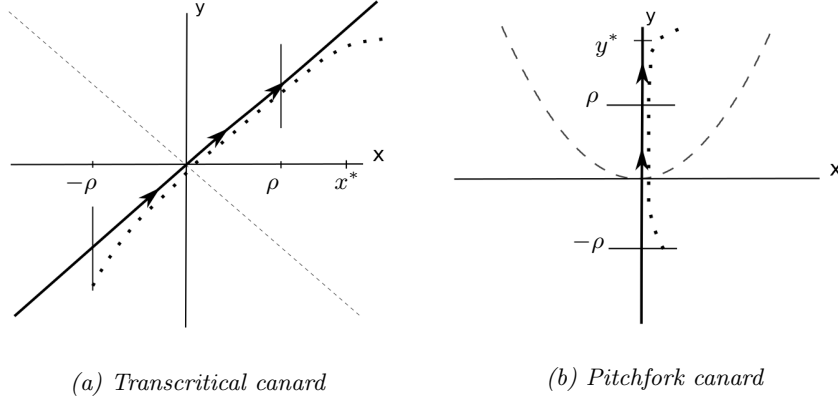


Figure 1: The sketches illustrate Theorem 1.1. The solid line with arrows indicates a canard, while the dotted curve is a nearby trajectory. The point  $x^*$  (resp.  $y^*$  for the pitchfork) indicates the  $x$ -coordinate where the contraction and the expansion along the canard have compensated each other. We show that, when an explicit RK-discretisation is employed, the delayed loss of stability in planar fast-slow maps with transcritical and pitchfork singularities is not symmetric (in contrast to their continuous time analogues). In fact the delay can be arbitrarily large. See more details in Section 2 and a numerical example in Section 4.

For ODEs of the form (1.1), the delay of bifurcation (for example for Hopf bifurcations [15, 24, 25]) can be characterised by the *way-in/way-out map* (or *input-output function*) derived in the following way (cf. [22, Section 12.2]): define the phase

$$\Phi(\tau) := \int_{\tau_*}^{\tau} \lambda_1(y^0(s)) ds,$$

where  $y^0(s)$  denotes the slow-flow solution for equation (1.1) and  $\tau_*$  is such that  $y^0(\tau_*) = 0$ , i.e. where  $y^0(s)$  is passing through the bifurcation point. Then for  $\tau$  sufficiently close to  $\tau_*$ , one can define the *way-in/way-out map*  $\Pi$  as the function that maps a time  $\tau < \tau_*$  to a time  $\Pi(\tau) > \tau_*$  by the condition

$$\operatorname{Re}[\Psi(\tau)] = \operatorname{Re}[\Psi(\Pi(\tau))]. \quad (1.7)$$

The essential statement of Theorem 1.1 is that for explicit Runge-Kutta discretisations of transcritical and pitchfork canards, the way-in/way-out map, which gives precisely  $\Pi(\tau) = \tau$  in the ODE situation, will explode for certain parameter regimes of  $\rho$  and  $h$ .

In the second part of the paper, we will see that the bilinear Kahan-Hirota-Kimura discretisation scheme, also abbreviated as *Kahan method* and known for preserving conserved quantities in various cases (see e.g. [27]), is more suitable for finding a way-in/way-out map with analogous properties to the ODE situation. We show in Section 3.1 that the Kahan method, which is in fact an implicit Runge-Kutta scheme that yields an explicit form for quadratic vector fields, preserves precisely the time-continuous structure of the transcritical canard in the sense, that the time trajectories spend at the attracting part of the canard is the same that they spend at the repelling part. In other words, the discrete-time way-in/way-out map, defined in analogy to (1.7), is completely symmetric in this case.

The Kahan method is not explicit in the case of the pitchfork singularity due to the cubic term which seems to make the analysis more cumbersome than before. However, we can still analyse the linearisation along the canard in this, now implicit, discretisation and obtain analogous results to the transcritical case. In the case of a folded canard, again the Kahan method turns out to be an accurate behaviour-preserving discretisation scheme for the canard problem [12]. In this case, an explicit Euler method does not even give a discrete-time canard trajectory such that the discrete-time dynamics could not be analysed as before. Hence, for the folded canard, we only focus on the Kahan map (see Section 2.3).

We can summarize the results on the symmetry of the way-in/way-out map for the Kahan discretisation of transcritical, pitchfork and fold singularities in the following Theorem, which is sketched in Figure 2.

**Theorem 1.2** (Symmetry for Kahan method). *For any  $h, \varepsilon > 0$  (except for one singular combination), consider the entry point  $x(0) = -\rho < 0$  (and  $y(0) = -\rho < 0$  in the pitchfork case).*

*If, in the case of the transcritical or pitchfork singularity, we have  $\rho = \varepsilon h N + \varepsilon h/2$  for some  $N \in \mathbb{N}$ , or in the case of the fold singularity we have  $\rho = \varepsilon h N/2$  for some  $N \in \mathbb{N}$ , then the way-in/way-out map  $\psi_h$  is well defined and takes the value*

$$\psi_h(-N) = N.$$

*Otherwise,*

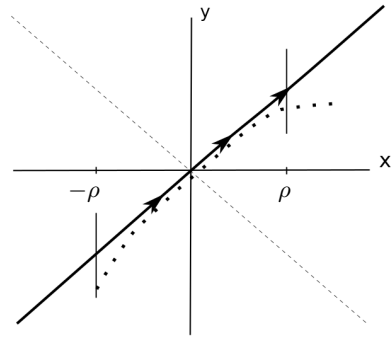
$$\psi_h(-N) \in \{N + 1, N + 2\}.$$

*In other words, the expansion has compensated for contraction at*

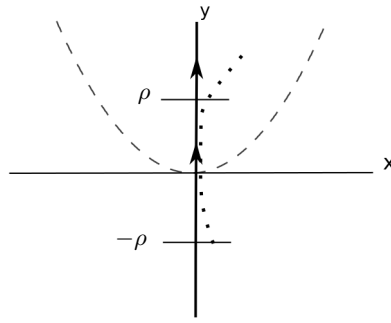
$$x^* \in \{\rho - \varepsilon h, \rho, \rho + \varepsilon h\}, \quad (y^* \in \{\rho - \varepsilon h, \rho, \rho + \varepsilon h\} \text{ in the pitchfork case})$$

*giving full symmetry of the entry-exit relation.*

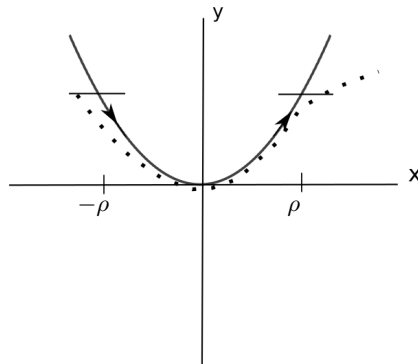
In the forthcoming Sections we prove Theorems 1.1 and 1.2. More specifically, Section 2 is dedicated to the analysis of fast-slow planar maps under explicit Runge-Kutta discretisation while in Section 3 we consider the Kahan-Hirota-Kimura scheme. Afterwards, in Section 4 we exemplify our theoretical results with a numerical simulation. We conclude this paper in Section 5 with a brief discussion.



(a) Transcritical canard



(b) Pitchfork canard



(c) Folded canard

Figure 2: The sketches illustrate Theorem 1.2. The solid curve with arrows indicates a canard, while the dotted curve is a nearby trajectory. We show that, when a Kahan discretisation scheme is employed, the delayed loss of stability in planar fast-slow maps with transcritical, pitchfork, and fold singularities is symmetric (in accordance with their continuous time analogues). See more details in Section 3 and a numerical example in Section 4.

## 2 Explicit Runge-Kutta Methods

This section is dedicated to the study of delayed loss of stability under explicit Runge-Kutta (RK) discretisation schemes. In order to clearly present the main ideas, we first consider a fast-slow transcritical singularity under a forward Euler discretisation, where we show the possibility of arbitrarily delayed loss of stability. Next, we show that the same conclusion holds for general explicit RK methods. Later we present a similar analysis for the pitchfork singularity.

### 2.1 Transcritical singularity

The canonical form (up to leading order terms) of the transcritical singularity in a fast-slow system reads as

$$\begin{aligned}x' &= x^2 - y^2 + \varepsilon, \\y' &= \varepsilon,\end{aligned}\tag{2.1}$$

where  $0 < \varepsilon \ll 1$  is the time scale separation parameter.

#### 2.1.1 Euler method

In this section we consider the iterated map obtained after forward-Euler discretisation of the canonical form of a fast-slow transcritical singularity, see [11] for the details. In particular, we consider the so-called canard case. To be precise, let us consider the map  $P : \mathbb{R}^2 \rightarrow \mathbb{R}^2$  given by

$$P(x, y) = (x + h(x^2 - y^2) + h\varepsilon, y + h\varepsilon),\tag{2.2}$$

where  $0 < \varepsilon \ll 1$ , and  $h > 0$ . We are interested in the dynamical system defined by iterations of the map  $P$ , that is  $P^n(x_0, y_0)$  where  $(x_0, y_0) \in \mathbb{R}^2$  are initial conditions and  $n \in \mathbb{N}$ . Note that the set  $S = \{x^2 = y^2\}$  is invariant under the iteration of  $P$ . In particular, the trajectory

$$\gamma(n) = (x_n, y_n) = (x_0 + nh\varepsilon, x_0 + nh\varepsilon), \quad n \in \mathbb{N},\tag{2.3}$$

corresponds to the “discrete-time maximal canard” in [11] and shall play an essential role in our analysis.

**Remark 2.1.** *Our goal is to give details on the contraction/expansion rate around  $\gamma$  in terms of  $(x_0, \varepsilon, h)$ . This is motivated by [11], where besides a thorough analysis of the fast-slow discrete time transcritical singularity, it is shown that the contraction towards the maximal canard is stronger in discrete time compared to its counterpart in continuous time, see [11, Theorem 3.1, (T3)].*

Proceeding with our analysis, we note that  $\gamma|_{\{\varepsilon=0\}}$  is attracting for  $x_0 < 0$  and repelling for  $x_0 > 0$ . Therefore, let  $\rho \in O(1)$  be a positive constant and set  $x_0 = -\rho$ . Next, we compute the variational equation of  $P^n$  along  $\gamma$ , which yields

$$v(n+1) = \begin{pmatrix} 1 + 2(-\rho + nh\varepsilon)h & -2(-\rho + nh\varepsilon)h \\ 0 & 1 \end{pmatrix} v(n),\tag{2.4}$$

where  $v(n) = (v_1(n), v_2(n)) \in \mathbb{R}^2$  and  $n \in \mathbb{N}$ . The local contraction/expansion rate is characterised by the solutions of (2.4) in the transversal (hyperbolic) direction, corresponding to the eigenvector

$(1, 0)^\top$ . Thus, the solution of (2.4) with initial condition  $(v_1(0), v_2(0)) = (1, 0)$  is given by  $(v_1(n), 0)$  where

$$v_1(n) = \prod_{k=0}^{n-1} (1 - 2h(\rho - kh\varepsilon)), \quad n \in \mathbb{N}, n > 0. \quad (2.5)$$

It is precisely the number given by  $v_1(n)$  that provides the overall contraction/expansion rate near  $\gamma$ . As an example, suppose that there exists a  $K \in \mathbb{N}$  that is the solution of

$$1 = \prod_{k=0}^{K-1} (1 - 2h(\rho - kh\varepsilon)). \quad (2.6)$$

Then  $K$  gives the number of iterations after which the contraction towards  $\gamma$  and the expansion away from  $\gamma$ , in the  $x$ -direction, have compensated each other. In other words, the time  $K$  is the discrete analogue of the *asymptotic moment of jumping* in continuous time. We can prove the following.

**Proposition 2.2.** *Consider the inequality*

$$\prod_{k=0}^{K-1} (1 - 2h(\rho - kh\varepsilon)) \geq 1, \quad (2.7)$$

where  $K \in \mathbb{N}$  and  $K > 1$ . If  $1 - 2h\rho > 0$  and the inequality holds, then

$$K \geq K^* = \frac{1}{h^2\varepsilon} \left( -1 + 2h\rho + \exp(W(-h^2\varepsilon \ln(1 - 2h\rho))) \right), \quad (2.8)$$

where  $W$  denotes the Lambert  $W$  function. Furthermore, let  $x^* = -\rho + K^*h\varepsilon$  for some fixed values of  $(h, \varepsilon)$ . Notice that  $x^*$  is the  $x$ -coordinate where the contraction/expansion rate around the canard is compensated. Then

$$\lim_{\rho \rightarrow \frac{1}{2h}} x^* = \infty. \quad (2.9)$$

*Proof.* To simplify the notations let  $a := 1 - 2h\rho > 0$ ,  $b := 2h^2\varepsilon > 0$ . Then (2.7) reads as

$$\prod_{k=0}^{K-1} (a + bk) \geq 1. \quad (2.10)$$

Taking the natural logarithm on both sides of (2.10), and isolating the term for  $k = 0$ , one gets

$$\sum_{k=1}^{K-1} \ln(a + bk) \geq -\ln(a). \quad (2.11)$$

Next, using the finite form of Jensen's inequality<sup>1</sup> one has

$$\ln \left( \frac{1}{K-1} \sum_{k=1}^{K-1} (a + bk) \right) \geq \frac{1}{K-1} \sum_{k=1}^{K-1} \ln(a + bk) \geq -\frac{1}{K-1} \ln(a). \quad (2.12)$$

---

<sup>1</sup>Let  $\phi$  be a real, concave function and  $\{x_i\}$  a sequence of numbers in the domain of  $\phi$ . Then the finite form of Jensen's inequality that we use is  $\phi \left( \frac{\sum \phi(x_i)}{n} \right) \geq \sum \frac{\phi(x_i)}{n}$ .

Hence, by disregarding the middle term in equation (2.12), and by simplifying the arithmetic series  $\sum_{k=1}^{K-1} a + bk$ , one obtains

$$K \ln \left( a + \frac{b}{2} K \right) > (K-1) \ln \left( a + \frac{b}{2} K \right) \geq -\ln(a). \quad (2.13)$$

Next, we disregard the middle term of the last inequality and define  $\exp(z) = a + \frac{b}{2} K$ , leading to

$$\exp(z)z > (\exp(z) - a)z > -\frac{b}{2} \ln(a), \quad (2.14)$$

where the last inequality holds due to  $a \in (0, 1)$ . Thus, it is clear that a lower bound for  $z$  is given by  $\exp(z^*)z^* = -\frac{b}{2} \ln(a)$ . Using the Lambert W function [9, Eq. 4.13] one gets  $z^* = W\left(-\frac{b}{2} \ln(a)\right)$ , which in turn provides a lower bound  $K^*$ , that is  $K \geq K^*$ , where

$$K^* = \frac{2}{b} \left( \exp \left( W \left( -\frac{b}{2} \ln(a) \right) \right) - a \right). \quad (2.15)$$

The proof is completed by re-substituting the values of  $a$  and  $b$ . The computation of the limit follows from the fact that  $\lim_{x \rightarrow \infty} W(x) = \infty$ .  $\square$

Next we extend the previous analysis to general explicit Runge-Kutta discretization schemes.

### 2.1.2 General explicit Runge-Kutta schemes

Given a planar system

$$\begin{aligned} x' &= f(x, y), \\ y' &= g(x, y), \end{aligned} \quad (2.16)$$

the  $s$ -stage *explicit* Runge-Kutta method is given by

$$\begin{aligned} x_{n+1} &= x_n + h \sum_{i=1}^s \alpha_i \kappa_i \\ y_{n+1} &= y_n + h \sum_{i=1}^s \alpha_i \ell_i, \end{aligned} \quad (2.17)$$

where

$$\begin{aligned} \kappa_i &= f \left( x_n + h \sum_{j=1}^{i-1} a_{ij} \kappa_j, y_n + h \sum_{j=1}^{i-1} a_{ij} \ell_j \right) \\ \ell_i &= g \left( x_n + h \sum_{j=1}^{i-1} a_{ij} \kappa_j, y_n + h \sum_{j=1}^{i-1} a_{ij} \ell_j \right), \end{aligned} \quad (2.18)$$

and the coefficients  $\alpha_i \in \mathbb{R}$  and  $a_{ij} \in \mathbb{R}$  depend on the RK-scheme and can be chosen from the so-called *Butcher tableau*. Thus, for a fast-slow system with a transcritical singularity (2.1) one has

$$\begin{aligned} x_{n+1} &= x_n + h \sum_{i=1}^s \alpha_i \kappa_i \\ y_{n+1} &= y_n + h \sum_{i=1}^s \alpha_i \ell_i, \end{aligned} \tag{2.19}$$

where  $\ell_i = \varepsilon$  and

$$\kappa_i = \left( x_n + h \sum_{j=1}^{i-1} a_{ij} \kappa_j \right)^2 - \left( y_n + h \varepsilon \sum_{j=1}^{i-1} a_{ij} \right)^2 + \varepsilon. \tag{2.20}$$

**Remark 2.3.** *The forward-Euler discretisation is the 1-stage explicit RK method.*

First we show that, similar to the Euler discretisation, the canard orbit  $\gamma(n) = (x_n, y_n) = (x_n, x_n)$  is a solution of the  $s$ -stage RK discretisation of the fast-slow transcritical singularity. To be more precise, from (2.19) let us consider the map  $P_s : \mathbb{R}^2 \rightarrow \mathbb{R}^2$  given by

$$P_s(x, y) = \left( x + h \sum_{i=1}^s \alpha_i \kappa_i, y + h \varepsilon \sum_{i=1}^s \alpha_i \right), \tag{2.21}$$

where

$$\kappa_i = \left( x + h \sum_{j=1}^{i-1} a_{ij} \kappa_j \right)^2 - \left( y + h \varepsilon \sum_{j=1}^{i-1} a_{ij} \right)^2 + \varepsilon. \tag{2.22}$$

It is clear that iterations of the map  $P_s$  define a discrete-time dynamical system. Next we show that, just as in the forward Euler case, the set  $S = \{(x, y) \in \mathbb{R}^2 \mid x = y\}$  is invariant under the iterations of  $P_s$  for any  $s \geq 1$ .

**Proposition 2.4.** *Consider (2.21). Then the set  $S = \{(x, y) \in \mathbb{R}^2 \mid x = y\}$  is invariant under the iterations of  $P_s$ . Moreover, if  $\sum_{i=1}^s \alpha_i = 1$ , then the solutions along  $S$  are given by  $\gamma_{x(0)}(n) = (x(0) + \varepsilon hn, x(0) + \varepsilon hn)$ .*

*Proof.* Let  $x = y$ , then from (2.22) it follows that

$$\kappa_i = 2xh \sum_{j=1}^{i-1} a_{ij} \kappa_j - 2xh\varepsilon \sum_{j=1}^{i-1} a_{ij} + h^2 \left( \sum_{j=1}^{i-1} a_{ij} \kappa_j \right)^2 - h^2 \varepsilon^2 \left( \sum_{j=1}^{i-1} a_{ij} \right)^2 + \varepsilon. \tag{2.23}$$

Note that  $\kappa_1 = \kappa_2 = \varepsilon$ . Next, assume that  $\kappa_1 = \dots = \kappa_{i-1} = \varepsilon$ . Then, it follows immediately from equation (2.23) that  $\kappa_i = \varepsilon$ , for all  $i = 1, \dots, s$ . This implies

$$P_s(x, x) = \left( x + h \varepsilon \sum_{i=1}^s \alpha_i, x + h \varepsilon \sum_{i=1}^s \alpha_i \right), \tag{2.24}$$

which shows that indeed the diagonal  $S$  is invariant. The expression of  $\gamma_{x(0)}(n)$  follows from the common assumption that  $\sum_{i=1}^s \alpha_i = 1$  which implies that  $y_{n+1} = y_n + h \sum_{i=1}^s \alpha_i \ell_i = y_n + h\varepsilon$ , and whose solutions are as indicated.  $\square$

Next, we are going to study the variational equation of (2.19) along  $\gamma_n$ . Thus, we have the following.

**Lemma 2.5.** *The variational equation of (2.19) along  $\gamma_n$  is given by*

$$v(n+1) = \begin{pmatrix} 1 + h \sum_{i=1}^s \alpha_i \frac{\partial \kappa_i}{\partial x_n} |_{\gamma_n} & h \sum_{i=1}^s \alpha_i \frac{\partial \kappa_i}{\partial y_n} |_{\gamma_n} \\ 0 & 1 \end{pmatrix} v(n). \quad (2.25)$$

Moreover the eigenvector corresponding to the eigenvalue 1 is  $(1, 1)^\top$ .

*Proof.* The Jacobian of (2.19) reads as

$$J = \begin{pmatrix} 1 + h \sum_{i=1}^s \alpha_i \frac{\partial \kappa_i}{\partial x_n} & h \sum_{i=1}^s \alpha_i \frac{\partial \kappa_i}{\partial y_n} \\ 0 & 1 \end{pmatrix}. \quad (2.26)$$

Recall that  $k_i|_{\gamma_n} = \varepsilon$ , and let  $A_i := \sum_{j=1}^{i-1} a_{ij}$ . Note that  $A_1 = 0$ . It follows that

$$\frac{\partial \kappa_i}{\partial x_n} |_{\gamma_n} = 2(x_n + h\varepsilon A_i) \left( 1 + h \sum_{j=1}^{i-1} a_{ij} \frac{\partial \kappa_j}{\partial x_n} |_{\gamma_n} \right), \quad (2.27)$$

$$\frac{\partial \kappa_i}{\partial y_n} |_{\gamma_n} = 2(x_n + h\varepsilon A_i) \left( -1 + h \sum_{j=1}^{i-1} a_{ij} \frac{\partial \kappa_j}{\partial y_n} |_{\gamma_n} \right). \quad (2.28)$$

Next, note that  $(1, 1)^\top$  is the eigenvector for the eigenvalue 1 of  $J|_{\gamma_n}$  if and only if  $\frac{\partial \kappa_i}{\partial y_n} |_{\gamma_n} = -\frac{\partial \kappa_i}{\partial x_n} |_{\gamma_n}$  for all  $i = 1, \dots, s$ . For  $i = 1$  this holds trivially, for the rest of the terms one proves the equality by induction.  $\square$

For notation convenience, let  $J_1(x_n)$  denote the first component of  $J|_{\gamma_n}$ , that is  $J_1(x_n) = 1 + hQ_s(x_n)$ , where, from (2.27), we have

$$Q_s(x_n) = \sum_{i=1}^s \alpha_i \frac{\partial \kappa_i}{\partial x_n} |_{\gamma_n} = \sum_{i=1}^s 2\alpha_i (x_n + h\varepsilon A_i) \left( 1 + h \sum_{j=1}^{i-1} a_{ij} \frac{\partial \kappa_j}{\partial x_n} |_{\gamma_n} \right) \quad (2.29)$$

**Remark 2.6.**  $Q_s(x_n)$  is, generically, a polynomial in  $x_n$  of degree  $s$ . Also, for sake of simplifying the notation, we are omitting the dependence of  $Q_s$  on  $(h, \varepsilon)$ .

Recall also that for initial condition  $x(0) = -\rho$ , the canard trajectory reads as  $\gamma_n = (x_n, y_n) = (-\rho + nh\varepsilon, -\rho + nh\varepsilon)$ . Just as in the Euler method  $J_1(-\rho)$  shall play an important role. In fact, let us define the following.

**Definition 2.7.** Let  $(\rho, h, \varepsilon) = (\rho^*, h^*, \varepsilon^*)$  be a solution of  $J_1(-\rho) = 0$ . Then we call  $(\rho^*, h^*, \varepsilon^*)$  a critical triplet.

**Remark 2.8.** For the forward Euler method the critical triplet is  $(\rho^*, h^*, \varepsilon^*) = (\frac{1}{2h}, h, \varepsilon)$ .

It follows from Lemma 2.5 that the centre eigenvector is aligned with the invariant space  $S$  along which the canard  $\gamma_n$  is located. Therefore, to study the contraction/expansion rate along  $\gamma_n$  we

consider the variational equation (2.25) in the transverse direction to  $(1, 1)^\top$ . For this, it suffices to consider (2.25) with initial condition  $v(0) = (1, 0)$ . Thus, with this setup, the solution  $v_1(n)$  of the variational equation (2.25) is given by

$$v_1(n) = \prod_{k=0}^{n-1} (1 + hQ_s(-\rho + kh\varepsilon)). \quad (2.30)$$

Note that (2.4) is obtained by choosing  $s = 1$  and the corresponding constants of the scheme in (2.30). Indeed for  $s = 1$ , one has  $\alpha_1 = 1$  and thus  $Q_s(-\rho) = -2\rho$ .

**Proposition 2.9.** *Consider the inequality*

$$\prod_{k=0}^{K-1} (1 + hQ_s(-\rho + kh\varepsilon)) \geq 1, \quad (2.31)$$

where  $K \in \mathbb{N}$  and  $K > 1$ . If  $1 + hQ_s(-\rho) > 0$ ,  $K > 2$ , and inequality (2.31) holds, then

$$K \geq K^* = 1 + \exp\left(W\left(-\frac{\log(1 + hQ_s(-\rho))}{\bar{C}(s+1)}\right)\right), \quad (2.32)$$

where  $W$  denotes the Lambert  $W$  function, and  $\bar{C}$  is a constant that is determined by the choice of the RK scheme. Assume that a critical triplet  $(\rho^*, h^*, \varepsilon^*)$  exists<sup>2</sup>. Then  $\lim_{(\rho, h, \varepsilon) \rightarrow (\rho^*, h^*, \varepsilon^*)} K^* = \infty$ . This means that if we define  $x^* = -\rho + K^*h\varepsilon$  (which is the  $x$ -coordinate at which the contraction/expansion rate is compensated), we have the limit

$$\lim_{(\rho, h, \varepsilon) \rightarrow (\rho^*, h^*, \varepsilon^*)} x^* = \infty. \quad (2.33)$$

*Proof.* Recalling Remark 2.6 and for simplicity of notation, let us write (2.31) as

$$\prod_{k=0}^{K-1} \sum_{i=0}^s \theta_i k^i \geq 1, \quad (2.34)$$

for some coefficients  $\theta_i = \theta_i(h, \varepsilon, R_s)$  where in  $R_s$  we gather the coefficients of the RK scheme. It is worth noting that  $\theta_0 = 1 + hQ_s(-\rho)$ . Taking log on both sides of (2.34) and proceeding similar to the proof of Proposition 2.2 we get

$$\sum_{k=1}^{K-1} \log\left(\sum_{i=0}^s \theta_i k^i\right) \geq -\log \theta_0. \quad (2.35)$$

Next, again using Jensen's inequality allows us to write

$$(K-1) \log\left(\frac{1}{K-1} \sum_{k=1}^{K-1} \sum_{i=1}^s \theta_i k^i\right) \geq -\log \theta_0. \quad (2.36)$$

---

<sup>2</sup>That is, the equation  $1 + hQ_s(-\rho) = 0$  has at least one real triplet solution.

Noting that the sums on the left side of equation (2.36) do commute, we then have

$$\begin{aligned} \sum_{k=1}^{K-1} \sum_{i=1}^s \theta_i k^i &= \sum_{i=1}^s \sum_{k=1}^{K-1} \theta_i k^i = \sum_{i=1}^s \theta_i \sum_{k=1}^{K-1} k^i \\ &= \sum_{i=1}^s \theta_i \left( \frac{1}{i+1} \sum_{j=0}^i \binom{i+1}{j} B_j (K-1)^{i+1-j} \right), \end{aligned} \quad (2.37)$$

where the last equality is obtained using Faulhaber's formula and the  $B_j$ 's are Bernoulli numbers of the second kind [6, pp. 106-109]. Substituting (2.37) in (2.36) leads to

$$(K-1) \log \left( \sum_{i=1}^s \theta_i \left( \frac{1}{i+1} \sum_{j=0}^i \binom{i+1}{j} B_j (K-1)^{i-j} \right) \right) \geq -\log \theta_0, \quad (2.38)$$

where we note that we have cancelled out the term  $\frac{1}{K-1}$  of the left hand side of (2.36) with the appropriate one in (2.37). For convenience let us write

$$\sum_{i=1}^s \theta_i \left( \frac{1}{i+1} \sum_{j=0}^i \binom{i+1}{j} B_j (K-1)^{i-j} \right) = \sum_{i=1}^s C_i (K-1)^i, \quad (2.39)$$

where  $C_i$ ,  $i = 1, \dots, n$ , are coefficients depending on  $(h, \varepsilon, R_s)$ . Next, note that for fixed  $s$  we have

$$\sum_{i=1}^s C_i (K-1)^i = \frac{\max\{|C_i|\}}{\max\{|C_i|\}} \sum_{i=1}^s C_i (K-1)^i = \max\{|C_i|\} \sum_{i=1}^s D_i (K-1)^i, \quad (2.40)$$

where  $D_i := \frac{C_i}{\max\{|C_i|\}} \in [-1, 1]$ . Hence, one has  $\max\{|C_i|\} \sum_{i=1}^s D_i (K-1)^i \leq \max\{|C_i|\} \sum_{i=1}^s (K-1)^i$  and therefore, simplifying the geometric series  $\sum_{i=1}^s (K-1)^i$  one gets

$$\sum_{i=1}^s C_i (K-1)^i \leq \max\{|C_i|\} \frac{(K-1)((K-1)^s - 1)}{K-2}. \quad (2.41)$$

One should keep in mind that the above geometric series is divergent, so one should fix a finite  $s$  for the above formula to make sense. In practical terms this is not an issue since we recall that  $s$  is the stage of the RK-method, and this is usually a small positive integer.

Combining (2.38) and (2.41), we get

$$(K-1) \log \left( \max\{|C_i|\} \underbrace{\frac{(K-1)((K-1)^s - 1)}{K-2}}_{=:F(K)} \right) \geq -\log \theta_0. \quad (2.42)$$

Note that  $F(K) > 2$  due to the fact that  $K > 2$ . Therefore:

$$\begin{aligned} \log(\max\{|C_i|\} F(K)) &= \left( \frac{\log(\max\{|C_i|\})}{\log(F(K))} + 1 \right) \log(F(K)) \\ &\leq \underbrace{\left( \frac{|\log(\max\{|C_i|\})|}{\log(2)} + 1 \right)}_{=:C} \log(F(K)). \end{aligned} \quad (2.43)$$

Furthermore, note that

$$\begin{aligned}\log(F(K)) &= \log\left(\frac{(K-1)((K-1)^s-1)}{K-2}\right) \\ &= \log((K-1)((K-1)^s-1)) - \log(K-2) \\ &\leq \log((K-1)^{s+1}) = (s+1)\log(K-1).\end{aligned}\tag{2.44}$$

So, combining (2.43) and (2.44) allows us to simplify (2.42) to

$$(K-1)\log(K-1) \geq -\frac{\log\theta_0}{\bar{C}(s+1)}.\tag{2.45}$$

Next, using the Lambert W function as we did for the proof of Proposition 2.2, we get the estimate

$$K \geq K^* = 1 + \exp\left(W\left(-\frac{\log\theta_0}{\bar{C}(s+1)}\right)\right).\tag{2.46}$$

Thus (2.32) follows from substituting the value of  $\theta_0 = 1 + hQ_s(-\rho)$  in (2.46). Finally, the argument for the limit of  $x^*$  follows from  $\lim_{x \rightarrow \infty} W(x) = \infty$ .  $\square$

**Remark 2.10.** *Although the proofs of Propositions 2.2 and 2.9 are similar, some of the intermediate simplifications are different. Hence, we do not recover the estimate (2.8) from (2.32).*

## 2.2 Pitchfork

The canonical form of the pitchfork singularity in a fast-slow system (up to leading order terms) reads

$$\begin{aligned}x' &= x(y - x^2) \\ y' &= \varepsilon,\end{aligned}\tag{2.47}$$

where, again,  $0 < \varepsilon \ll 1$  is the time scale separation parameter.

The analysis of the expansion-contraction rate for the fast-slow pitchfork singularity under forward Euler discretisation is similar to the one performed for the transcritical singularity. Therefore, we just sketch the main arguments, see [1] for the details.

The map obtained after forward Euler discretisation of the fast-slow pitchfork singularity is given by

$$P(x, y) = (x + h(x(y - x^2)), y + h\varepsilon).\tag{2.48}$$

In this case the canard trajectory is

$$\gamma(n) = (0, y_0 + nh\varepsilon), \quad n \in \mathbb{N}.\tag{2.49}$$

Letting  $y_0 = -\rho$ , where  $\rho \in \mathcal{O}(1)$  is a positive constant we find that the expansion-contraction rate along  $\gamma$  is given by (compare with (2.5))

$$v_1(n) = \prod_{k=0}^{n-1} (1 + h(-\rho^2 + kh\varepsilon)).\tag{2.50}$$

Then, analogously to Proposition 2.2, for the pitchfork case we have the following.

**Proposition 2.11.** *Consider the inequality*

$$\prod_{k=0}^{K-1} (1 + h(-\rho^2 + kh\varepsilon)) \geq 1, \quad (2.51)$$

where  $K \in \mathbb{N}$  and  $K > 1$ . If  $1 - h\rho^2 > 0$  and inequality (2.51) holds, then

$$K \geq K^* := \frac{1}{h^2\varepsilon} (-1 + h\rho^2 + \exp(W(-h^2\varepsilon \ln(1 - h\rho^2))))), \quad (2.52)$$

where  $W$  denotes the Lambert  $W$  function. Furthermore, let  $y^* = -\rho + K^*h\varepsilon$ , then

$$\lim_{\rho \rightarrow \sqrt{\frac{1}{h}}} y^* = \infty. \quad (2.53)$$

*Proof.* The proof follows the exact same reasoning as the proof of Proposition 2.2, so we do not repeat it here.  $\square$

**Remark 2.12.** *Again, just as we elaborated for the transcritical singularity, the arbitrarily delayed loss of stability holds for general explicit Runge-Kutta methods. We omit the details here as the reasoning is very similar to Section 2.1.2.*

## 2.3 Fold

We consider the canonical form of a fold singularity in a fast-slow system

$$\begin{aligned} x' &= -y + x^2, \\ y' &= \varepsilon x. \end{aligned} \quad (2.54)$$

where  $0 < \varepsilon \ll 1$  again quantifies the time scale separation.

We apply the explicit Euler discretisation with step size  $h > 0$  to system (2.54) and obtain the map  $P_E : \mathbb{R}^2 \rightarrow \mathbb{R}^2$  given by

$$P_E : \begin{pmatrix} x \\ y \end{pmatrix} \mapsto \begin{pmatrix} \tilde{x} \\ \tilde{y} \end{pmatrix} = \begin{pmatrix} x + h(x^2 - y) \\ y + \varepsilon hx \end{pmatrix}. \quad (2.55)$$

Note that by the change of variables  $\varepsilon h \rightarrow h$  we can write the system in the slow time scale as

$$\varepsilon \frac{\tilde{x} - x}{h} = x^2 - y, \quad \frac{\tilde{y} - y}{h} = x. \quad (2.56)$$

In analogy to the time-continuous case, the critical manifold  $\mathcal{S}$  is given as

$$\mathcal{S} = \{(x, y) \in \mathbb{R}^2 : y = x^2\},$$

splitting into two normally hyperbolic branches, the attracting subset  $\mathcal{S}_a = \{(x, y) \in \mathcal{S} : x < 0\}$  and the repelling subset  $\mathcal{S}_r = \{(x, y) \in \mathcal{S} : x > 0\}$ . It follows from [16, Theorem 4.1] that for  $\varepsilon, h > 0$  small enough there are corresponding forward invariant slow manifolds  $\mathcal{S}_{a,\varepsilon,h}$  and  $\mathcal{S}_{r,\varepsilon,h}$ . The origin, i.e. the canard point in the ODE case, is again a non-hyperbolic singularity.

However, we make the following observation (which is a simplified version of [12, Proposition 3.1]):

**Proposition 2.13.** *The equation of the slow subsystem corresponding with (2.56) reads*

$$\tilde{x}^2 = x^2 + xh,$$

which has the two solutions

$$\tilde{x} = \pm\sqrt{x^2 + xh},$$

on the set

$$\{(x, y) \in (\mathbb{R} \setminus (-h, 0)) \times \mathbb{R} : y = x^2\} \subset S.$$

Each solution has a fixed point at  $x = 0$  as opposed to the continuous-time case where the slow flow follows  $\dot{x} = \frac{1}{2}$ .

*Proof.* Setting  $\varepsilon = 0$  in (2.56), the statement follows from a straight forward calculation.  $\square$

This shows that there is no canard solution on  $S$  through the origin and we cannot expect the occurrence of canards for any explicit Runge-Kutta scheme.

Additionally, when  $\varepsilon > 0$ , we observe that (cf. [12, Remark 2.2]) the ODE system (2.54) possesses the conserved quantity

$$H(x, y) = \frac{1}{2}e^{-2y/\varepsilon} \left( y - x^2 + \frac{\varepsilon}{2} \right), \quad (2.57)$$

vanishing on the invariant set

$$\mathcal{S}_\varepsilon := \left\{ (x, y) \in \mathbb{R}^2 : y = x^2 - \frac{\varepsilon}{2} \right\}, \quad (2.58)$$

which consists precisely of the attracting branch  $\mathcal{S}_{a,\varepsilon} = \{(x, y) \in \mathcal{S}_\varepsilon : x < 0\}$  and the repelling branch  $\mathcal{S}_{r,\varepsilon} = \{(x, y) \in \mathcal{S}_\varepsilon : x > 0\}$ , such that trajectories on  $\mathcal{S}_\varepsilon$  go through the origin with speed  $\dot{x} = \varepsilon/2$ . Similarly to Proposition 2.13, it follows from an easy calculation that there is no function  $c(\varepsilon, h)$  such that  $\{y = x^2 - \frac{\varepsilon}{2} + c(\varepsilon, h)\}$  is invariant for the dynamics induced by (2.55).

Clearly, we have to use a different, structure-preserving discretisation if we want to understand a canard solution for the fold case in discrete-time. This is another motivation for considering the Kahan-Hirota-Kimura scheme, introduced in the next chapter.

### 3 Kahan-Hirota-Kimura Scheme

We consider a method that has produced *integrable* maps in several examples, i.e. maps that conserve a certain quantity: the Kahan-Hirota-Kimura discretisation scheme (see e.g. [27]) was introduced by Kahan in the unpublished lecture notes [20] for ODEs with quadratic vector fields

$$\dot{z} = f(z) = Q(z) + Bz + c, \quad (3.1)$$

where each component of  $Q : \mathbb{R}^n \rightarrow \mathbb{R}^n$  is a quadratic form,  $B \in \mathbb{R}^{n \times n}$  and  $c \in \mathbb{R}^n$ . The Kahan-Hirota-Kimura discretisation, short *Kahan method*, reads as

$$\frac{\tilde{z} - z}{h} = \bar{Q}(z, \tilde{z}) + \frac{1}{2}B(z + \tilde{z}) + c, \quad (3.2)$$

where

$$\bar{Q}(z, \tilde{z}) = \frac{1}{2}(Q(z + \tilde{z}) - Q(z) - Q(\tilde{z}))$$

is the symmetric bilinear form such that  $\bar{Q}(z, z) = Q(z)$ . Note that equation (3.2) is linear with respect to  $\tilde{z}$  and by that defines a *rational* map  $\tilde{z} = \Lambda_f(z, h)$ , which approximates the time  $h$  shift along the solutions of the ODE (3.1). Further note that  $\Lambda_f^{-1}(z, h) = \Lambda_f(z, -h)$  and, hence, the map is *birational*.

The explicit form of the map  $\Lambda_f$  defined by equation (3.2) is given as

$$\tilde{z} = \Lambda_f(z, h) = z + h \left( \text{Id} - \frac{h}{2} \text{D}f(z) \right)^{-1} f(z). \quad (3.3)$$

The Kahan method is the specific form, for quadratic vector fields, of an implicit Runge-Kutta scheme which is given by (cf. [5, Proposition 1])

$$\frac{\tilde{z} - z}{h} = -\frac{1}{2}f(z) + 2f\left(\frac{z + \tilde{z}}{2}\right) - \frac{1}{2}f(\tilde{z}). \quad (3.4)$$

Note that the ODE (2.47) has a cubic term which will make it necessary to use the general form (3.4).

### 3.1 Transcritical

The Kahan discretisation of equation (2.1) gives the map  $P_K : \mathbb{R}^2 \setminus \{x = \frac{1}{h}\} \rightarrow \mathbb{R}^2$ , written as

$$P_K(x, y) = \begin{pmatrix} \tilde{x}(x, y) \\ \tilde{y}(x, y) \end{pmatrix} = \begin{pmatrix} \frac{x + \varepsilon h - hy(y + \varepsilon h)}{1 - hx} \\ y + \varepsilon h \end{pmatrix}, \quad (3.5)$$

where  $0 < \varepsilon \ll 1$ , and  $h > 0$ .

Similarly to the continuous-time and the Runge-Kutta case, we find the diagonal to be an invariant curve for (3.5) with special canard solution  $\gamma$ . In more detail, we have the following statements:

**Proposition 3.1.** *The diagonal*

$$S := \{(x, y) \in \mathbb{R}^2 : y = x\} \quad (3.6)$$

*is invariant under iterations of  $P_K$  (3.5). Solutions on  $S$  are given by*

$$\gamma_{x(0)}(n) = (x(0) + \varepsilon hn, x(0) + \varepsilon hn), \forall n \in \mathbb{Z}. \quad (3.7)$$

*In particular, for  $(x, y) \in S$  we have:*

$$\left| \frac{\partial \tilde{x}}{\partial x} \right| \begin{cases} < 1 & \text{as long as } x < -\varepsilon h/2, \\ = 1 & \text{for } x = -\varepsilon h/2, \\ > 1 & \text{as long as } x > -\varepsilon h/2, x \neq 1/h. \end{cases} \quad (3.8)$$

*A special canard solution, symmetric with respect to the partition*

$$S = S_a \cup \{(-\varepsilon h/2, -\varepsilon h/2)\} \cup S_r,$$

*where*

$$S_a = \{(x, y) \in S : x < -\varepsilon h/2\}, \quad S_r = \{(x, y) \in S : x > -\varepsilon h/2\}, \quad (3.9)$$

*is given for  $x(0) = -\varepsilon h/2$  and denoted by*

$$\gamma(n) = \left( \varepsilon h \frac{2n-1}{2}, \varepsilon h \frac{2n-1}{2} \right), \forall n \in \mathbb{Z}. \quad (3.10)$$

*Proof.* The invariance of  $S$  follows from an easy calculation. Furthermore, observe that if  $(x, y) \in S$ , we have

$$\tilde{x} = \frac{x - hx^2 + \varepsilon h - \varepsilon h^2 x}{1 - hx} = \frac{x(1 - hx) + \varepsilon h(1 - hx)}{1 - hx} = x + \varepsilon h.$$

We compute the Jacobian matrix associated with (3.5) as

$$\frac{\partial(\tilde{x}, \tilde{y})}{\partial(x, y)} = \begin{pmatrix} \frac{1 - h^2 y(y + \varepsilon h) + \varepsilon h^2}{(1 - hx)^2} & \frac{-2hx - \varepsilon h^2}{1 - hx} \\ 0 & 1 \end{pmatrix}. \quad (3.11)$$

In particular, observe that

$$\begin{aligned} \frac{\partial \tilde{x}}{\partial x}(x, y)|_{(x, y) \in S} &= \frac{1 - h^2 y(y + \varepsilon h) + \varepsilon h^2}{(1 - hx)^2} \Big|_{(x, y) \in S} \\ &= \frac{1 - h^2 x^2 - x\varepsilon h^3 + \varepsilon h^2}{(1 - hx)^2} =: \frac{f_h(x)}{g_h(x)} =: J_h(x). \end{aligned} \quad (3.12)$$

It is easy to calculate that  $J_h(-\varepsilon h/2) = 1$ .

The parabolas given by the graphs of  $f_h$  and  $g_h$  intersect at  $x = -\varepsilon h/2$ , where  $f_h$  has a maximum, and  $x = \frac{1}{h}$ , where  $g_h$  has a minimum, as can be easily seen from the derivatives  $f'_h(x) = -2h^2 x - \varepsilon h^3$  and  $g'_h(x) = 2h^2 x - 2h$  (and the second derivatives). Hence, for  $x < -\varepsilon h/2$ , we have  $|g'_h(x)| > |f'_h(x)|$  and, in particular,  $|g_h(x)| > |f_h(x)|$ . For  $1/h > x > -\varepsilon h/2$ , we clearly have that  $f_h(x) > g_h(x) > 0$  according to the observations above. Furthermore, for  $x > 1/h$ , we have  $|f'_h(x)| > |g'_h(x)|$  and therefore  $|f_h(x)| > |g_h(x)|$ . This shows the claim (3.8).

The existence of the special canard  $\gamma$  (3.10) then follows directly.  $\square$

We denote the second entry of the matrix (3.11) by

$$\tilde{J}_h(x) := \frac{-2hx - \varepsilon h^2}{1 - hx}.$$

Similarly to the Runge-Kutta case discussed in Section 2.1, let  $\rho \in O(1)$  be a positive constant and set  $x(0) = -\rho$ . The variational equation of  $P_K^n$  along  $\gamma_{h, -\rho}$  reads

$$v(n+1) = \begin{pmatrix} J_h(-\rho + \varepsilon hn) & \tilde{J}_h(-\rho + \varepsilon hn) \\ 0 & 1 \end{pmatrix} v(n), \quad (3.13)$$

where  $v(n) = (v_1(n), v_2(n)) \in \mathbb{R}^2$  and  $n \in \mathbb{N}$ . It follows from an easy calculation that the matrix (3.12) has a simple eigenvalue 1 for the eigenvector  $(1, 1)^\top$  which is a fixed point of equation (3.13) and characterises the normal direction along the canard. The local contraction/expansion rate is characterised by the solutions of (3.13) in the transversal (hyperbolic) direction, corresponding to the eigenvector  $(1, 0)^\top$ . Thus, the solution of (3.13) with initial condition  $(v_1(0), v_2(0)) = (1, 0)$  is given by  $(v_1(n), 0)$ , where

$$v_1(n) = \prod_{k=0}^n J_h(-\rho + \varepsilon hk) \quad \forall n \geq 0.$$

When  $\rho = \varepsilon h N + \varepsilon h/2$  for some  $N \in \mathbb{N}$ , then  $\gamma_{-\rho} = \gamma$ , i.e. we are on the special canard (3.10). In this case, we can use the symmetry around  $-\varepsilon h/2$ , define

$$\begin{aligned} v^*(m) &:= \prod_{k=0}^m J_h\left(\varepsilon h \frac{2k-1}{2}\right) \quad \forall m \geq 0, \\ v^*(m) &:= \prod_{k=m}^0 J_h\left(\varepsilon h \frac{2k-1}{2}\right) \quad \forall m \leq 0, \end{aligned} \tag{3.14}$$

and observe that for all  $n \geq N$

$$v_1(n) = v^*(-N)v^*(n-N). \tag{3.15}$$

This leads to the following statement concerning contraction and expansion along the canard solutions:

**Proposition 3.2.** *For any  $h, \varepsilon > 0$  such that  $\frac{1}{\varepsilon h^2} + \frac{1}{2} \notin \mathbb{N}$ , consider the entry point  $x(0) = -\rho < 0$ .*

1. *If  $\rho = \varepsilon h N + \varepsilon h/2$  for some  $N \in \mathbb{N}$ , then the way-in/way-out map  $\psi_h$  given by*

$$\begin{aligned} 1 &= \prod_{k=0}^{N+\psi_h(-N)} |J_h(-\rho + \varepsilon h k)| = |v_1(N + \psi_h(-N))| \\ &= |v^*(-N)v^*(\psi_h(-N))|, \end{aligned}$$

*is well defined and takes the value*

$$\psi_h(-N) = N.$$

*In other words, the accumulated contraction and expansion rates compensate each other in perfect symmetry.*

2. *If, generally,  $\rho \in (\varepsilon h N + \varepsilon h/2, \varepsilon h(N+1) + \varepsilon h/2)$  for some  $N \in \mathbb{N}$  such that  $(\frac{1}{h}, \frac{1}{h}) \notin \gamma_{-\rho}$ , then the way-in/way-out map  $\psi_h(-N)$  is given by the smallest natural number such that*

$$1 \leq \prod_{k=0}^{N+\psi_h(-N)} |J_h(-\rho + \varepsilon h k)| = |v_1(N + \psi_h(-N))|,$$

*and satisfies*

$$\psi_h(-N) \in \{N+1, N+2\}. \tag{3.16}$$

*Summarising both cases, we conclude that the expansion has compensated for contraction at*

$$x^* \in \{\rho - \varepsilon h, \rho, \rho + \varepsilon h\},$$

*giving full symmetry of the entry-exit relation.*

*Proof.* It follows from a tedious but straight-forward calculation that

$$J_h\left(\varepsilon h \frac{2n-1}{2}\right) J_h\left(\varepsilon h \frac{-2n-1}{2}\right) = 1$$

for all  $\varepsilon h \frac{2n-1}{2} \neq 1/h$ ,  $n \in \mathbb{Z}$ . Hence, the first claim follows immediately.

For the second claim: firstly, observe that  $J_h$  is strictly increasing for all  $x \neq 1/h$ , since we obtain with equation (3.12) that

$$J_h(x)' = \frac{f_h'(x)g_h(x) - g_h'(x)f_h(x)}{g_h(x)^2} = \frac{h(2 + \varepsilon h^2)}{(1 - hx)^2} > 0.$$

Hence, we can estimate

$$\prod_{k=0}^{N+N+2} |J_h(-\rho + \varepsilon hk)| \geq v_1(N)v^*(N+1) \geq v^*(-(N+1))v^*(N+1) = 1$$

Therefore we can deduce  $\psi_h(-N) \leq N+2$ . Furthermore, we get directly from the strictly monotonic increase of  $J_h$  that

$$\prod_{k=0}^{N+N} |J_h(-\rho + \varepsilon hk)| < v^*(-N)v^*(N) = 1,$$

such that  $\psi_h(-N) > N$  follows. This finishes the proof.  $\square$

**Remark 3.3.** *Contraction and expansion balance out completely along the canard solution for the Kahan map which mirrors exactly the time-continuous case where*

$$v^*(\rho) = \int_0^\rho 2x \, dx,$$

such that the way-in/way-out map  $\psi$  satisfies  $\psi(\rho) = -\rho$  for all  $\rho \in I \subset \mathbb{R}$  for some appropriate interval  $I$ . We can make the starting and end point of the time-continuous and time-discrete system coincide exactly when simply choosing  $\rho = \varepsilon h \frac{2n-1}{2}$  for some  $n \in \mathbb{N}$ .

## 3.2 Pitchfork

We now consider the Kahan discretisation of equation (2.47), according to the implicit scheme (3.4). Note that, due to the cubic term, discretisation (3.2) is not applicable.

The scheme gives the equations

$$\frac{\tilde{x} - x}{h} = -\frac{1}{2}(xy - x^3) + 2 \left[ \frac{x + \tilde{x}}{2} \frac{y + \tilde{y}}{2} - \frac{(x + \tilde{x})^3}{8} \right] - \frac{1}{2}(\tilde{x}\tilde{y} - \tilde{x}^3), \quad (3.17a)$$

$$\frac{\tilde{y} - y}{h} = \varepsilon. \quad (3.17b)$$

As opposed to the transcritical case, we do not obtain an explicit map but possibly several solutions. When we start with  $x = 0$  and  $y \in (-\infty, 2/h)$ , we get

$$\tilde{x} \in \left\{ -\sqrt{\frac{4-2hy}{h}}, 0, \sqrt{\frac{4-2hy}{h}} \right\}$$

from equation (3.17). We can still analyse a canard solution in the following way:

**Proposition 3.4.** *The set*

$$S := \{(x, y) \in \mathbb{R}^2 : x = 0\} \quad (3.18)$$

*is invariant under particular solutions of equations (3.17) which are given by*

$$\gamma_{h,y(0)}(n) = (0, y(0) + \varepsilon hn), \forall n \in \mathbb{Z}. \quad (3.19)$$

*In particular, for  $(x, y) \in S$  we have:*

$$\left| \frac{\partial \tilde{x}}{\partial x} \right| \begin{cases} < 1 & \text{as long as } y < -\varepsilon h/2, \\ = 1 & \text{for } y = -\varepsilon h/2, \\ > 1 & \text{as long as } y > -\varepsilon h/2, y \neq 2/h. \end{cases} \quad (3.20)$$

*A special Canard solution, symmetric with respect to the partition*

$$S = S_a \cup \{(0, -\varepsilon h/2)\} \cup S_r,$$

*where*

$$S_a = \{(x, y) \in S : y < -\varepsilon h/2\}, \quad S_r = \{(x, y) \in S : y > -\varepsilon h/2\}, \quad (3.21)$$

*is given for  $y(0) = -\varepsilon h/2$  and denoted by*

$$\gamma(n) = \left(0, \varepsilon h \frac{2n-1}{2}\right), \forall n \in \mathbb{Z}. \quad (3.22)$$

*Proof.* The existence of trajectories  $\gamma_{h,y(0)}$  on  $S$  follows from an easy calculation. Furthermore, observe that

$$\begin{aligned} \frac{1}{h} \frac{\partial \tilde{x}}{\partial x} &= \frac{1}{h} - \frac{1}{2}y + \frac{3}{2}x^2 + \frac{1}{2}(y + \tilde{y}) + \frac{1}{2}(y + \tilde{y}) \frac{\partial \tilde{x}}{\partial x} \\ &\quad - \frac{1}{4} \left( 3x^2 + 3\tilde{x}^2 \frac{\partial \tilde{x}}{\partial x} + 6x\tilde{x} + 3x^2 \frac{\partial \tilde{x}}{\partial x} + 3\tilde{x}^2 + 6x\tilde{x} \frac{\partial \tilde{x}}{\partial x} \right) - \frac{1}{2}\tilde{y} \frac{\partial \tilde{x}}{\partial x} + \frac{3}{2}\tilde{x}^2 \frac{\partial \tilde{x}}{\partial x}. \end{aligned}$$

Hence, at  $x = \tilde{x} = 0$ , we obtain

$$\frac{\partial \tilde{x}}{\partial x} = 1 + \frac{h}{2}\tilde{y} + \frac{h}{2}y \frac{\partial \tilde{x}}{\partial x},$$

which gives

$$\frac{\partial \tilde{x}}{\partial x}(x, y)|_{(x,y) \in S} = \frac{1 + \frac{h}{2}y + \frac{h^2}{2}\varepsilon}{1 - \frac{h}{2}y} =: J_h(y). \quad (3.23)$$

Similarly to the transcritical case, one can compute that  $J_h(-\varepsilon h/2) = 1$  and

$$J'_h(y) = \frac{h + \frac{h^3\varepsilon}{4}}{(1 - \frac{h}{2}y)^2} > 0, \quad \forall y \neq \frac{2}{h}.$$

The existence of the special canard  $\gamma$  (3.22) then follows directly.  $\square$

Similarly to the transcritical case, let  $\rho \in O(1)$  be a positive constant and set  $y(0) = -\rho$ . It is easy to compute

$$\frac{\partial \tilde{x}}{\partial y}(x, y)|_{(x,y) \in S} = 0.$$

Hence, the variational equation along  $\gamma_{-\rho}$  reads

$$v(n+1) = \begin{pmatrix} J_h(-\rho + \varepsilon hn) & 0 \\ 0 & 1 \end{pmatrix} v(n), \quad (3.24)$$

where  $v(n) = (v_1(n), v_2(n)) \in \mathbb{R}^2$  and  $n \in \mathbb{N}$ . The Jacobian matrix has a simple eigenvalue 1 for the eigenvector  $(0, 1)^\top$  which is a fixed point of equation (3.24) and characterises the normal direction along the canard. The local contraction/expansion rate is characterised by trajectories in the transversal (hyperbolic) direction, corresponding to the eigenvector  $(1, 0)^\top$ . Thus, the solution of (3.24) with initial condition  $(v_1(0), v_2(0)) = (1, 0)$  is given by  $(v_1(n), 0)$ , where

$$v_1(n) = \prod_{k=0}^n J_h(-\rho + \varepsilon hk) \quad \forall n \geq 0.$$

When  $\rho = \varepsilon hN + \varepsilon h/2$  for some  $N \in \mathbb{N}$ , then  $\gamma_{h, -\rho} = \gamma$ , i.e. we are on the special canard (3.22). As before, we introduce

$$\begin{aligned} v^*(m) &:= \prod_{k=0}^m J_h(\varepsilon h \frac{2k-1}{2}) \quad \forall m \geq 0, \\ v^*(m) &:= \prod_{k=m}^0 J_h(\varepsilon h \frac{2k-1}{2}) \quad \forall m \leq 0, \end{aligned} \quad (3.25)$$

and observe that for all  $n \geq N$

$$v_1(n) = v^*(-N)v^*(n-N). \quad (3.26)$$

This leads to the following statement, analogously to Proposition 3.2:

**Proposition 3.5.** *For any  $h, \varepsilon > 0$  such that  $\frac{2}{\varepsilon h^2} + \frac{1}{2} \notin \mathbb{N}$ , consider the entry point  $y(0) = -\rho < 0$ .*

1. *If  $\rho = \varepsilon hN + \varepsilon h/2$  for some  $N \in \mathbb{N}$ , then the way-in/way-out map  $\psi_h$  given by*

$$\begin{aligned} 1 &= \prod_{k=0}^{N+\psi_h(-N)} |J_h(-\rho + \varepsilon hk)| = |v_1(N + \psi_h(-N))| \\ &= |v^*(-N)v^*(\psi_h(-N))|, \end{aligned}$$

*is well defined and takes the value*

$$\psi_h(-N) = N.$$

*In other words, the accumulated contraction and expansion rates compensate each other in perfect symmetry.*

2. *If, generally,  $\rho \in (\varepsilon hN + \varepsilon h/2, \varepsilon h(N+1) + \varepsilon h/2)$  for some  $N \in \mathbb{N}$  such that  $(0, \frac{2}{h}) \notin \gamma_{-\rho}$ , then the way-in/way-out map  $\psi_h(-N)$  is given by the smallest natural number such that*

$$1 \leq \prod_{k=0}^{N+\psi_h(-N)} |J_h(-\rho + \varepsilon hk)| = |v_1(N + \psi_h(-N))|,$$

*and satisfies*

$$\psi_h(-N) \in \{N+1, N+2\}. \quad (3.27)$$

Summarising both cases, we conclude that the expansion has compensated for contraction at

$$y^* \in \{\rho - \varepsilon h, \rho, \rho + \varepsilon h\},$$

giving full symmetry of the entry-exit relation.

*Proof.* Similarly to the transcritical case, we observe that

$$J_h \left( \varepsilon h \frac{2n-1}{2} \right) J_h \left( \varepsilon h \frac{-2n-1}{2} \right) = 1$$

for all  $\varepsilon h \frac{2n-1}{2} \neq 2/h$ ,  $n \in \mathbb{Z}$ . Hence, the first claim follows immediately. The second claim can be deduced from arguments analogously to the proof of Proposition 3.2.  $\square$

In the transcritical and pitchfork case, the canards are given on lines and we observe the same linear structure for the Kahan discretisations in both situations, with exactly the same symmetry properties. We will turn to the problem of a folded canard in the next subsection.

### 3.3 Fold

In contrast to [12], we will restrict the following analysis to the most basic canonical form of a fast-slow system with fold singularity, i.e. model (2.54), since we are only interested in the properties of the linearisation along the canard solution.

The Kahan discretisation of system (2.54) reads as

$$\frac{\tilde{x} - x}{h} = \tilde{x}x - \frac{\tilde{y} + y}{2}, \quad \frac{\tilde{y} - y}{h} = \varepsilon \frac{\tilde{x} + x}{2}, \quad (3.28)$$

and induces the invertible, birational map  $P_K : \mathbb{R}^2 \rightarrow \mathbb{R}^2$ , written explicitly as

$$P_K : \begin{pmatrix} x \\ y \end{pmatrix} \mapsto \begin{pmatrix} \tilde{x} \\ \tilde{y} \end{pmatrix} = \begin{pmatrix} \frac{x - hy - \frac{h^2}{4}\varepsilon x}{1 - hx + \frac{h^2}{4}\varepsilon} \\ \frac{y - hyx - \frac{h^2}{2}\varepsilon x^2 + h\varepsilon x - \frac{h^2}{4}\varepsilon y}{1 - hx + \frac{h^2}{4}\varepsilon} \end{pmatrix}. \quad (3.29)$$

Similarly to before, we make the following observations (which can be found in a similar form in [12]):

**Proposition 3.6.** *The parabola*

$$S := \left\{ (x, y) \in \mathbb{R}^2 : y = x^2 - \frac{\varepsilon}{2} - \frac{\varepsilon^2 h^2}{8} \right\} \quad (3.30)$$

is invariant under iterations of  $P_K$  (3.29). Solutions on  $S$  are given by

$$\gamma_{x(0)}(n) = \left( x(0) + n \frac{\varepsilon h}{2}, \left( x(0) + n \frac{\varepsilon h}{2} \right)^2 - \frac{\varepsilon}{2} - \frac{\varepsilon^2 h^2}{8} \right), \forall n \in \mathbb{Z}, \quad (3.31)$$

For  $(x, y) \in S$  we have

$$\left| \frac{\partial \tilde{x}}{\partial x} \right| \begin{cases} < 1 & \text{as long as } x < 0, \\ = 1 & \text{for } x = 0, \\ > 1 & \text{as long as } x > 0, x \neq \left(1 + \frac{h^2 \varepsilon}{4}\right) / h. \end{cases} \quad (3.32)$$

A special Canard solution, symmetric with respect to the partition

$$S = S_a \cup \{(0, 0)\} \cup S_r,$$

where

$$S_a = \{(x, y) \in S : x < 0\}, \quad S_r = \{(x, y) \in S : x > 0\}, \quad (3.33)$$

is given for  $x(0) = 0$  and denoted by

$$\gamma_h(n) = \left( n \frac{\varepsilon h}{2}, \left( n \frac{\varepsilon h}{2} \right)^2 - \frac{\varepsilon}{2} - \frac{\varepsilon^2 h^2}{8} \right), \quad \forall n \in \mathbb{Z}. \quad (3.34)$$

*Proof.* The invariance of  $S$  follows from a cumbersome but straight-forward calculation, checking that for

$$y = x^2 - \frac{\varepsilon}{2} - \frac{\varepsilon^2 h^2}{8},$$

we indeed have

$$\tilde{y} = \tilde{x}^2 - \frac{\varepsilon}{2} - \frac{\varepsilon^2 h^2}{8}.$$

Furthermore, observe that if  $(x(0), y(0)) \in S$ , we have

$$\tilde{x} = \frac{x - hx^2 + \frac{\varepsilon h}{2} + \frac{\varepsilon^2 h^3}{8} - \frac{h^2 \varepsilon}{4} x}{1 - hx + \frac{h^2}{4} \varepsilon} = \frac{\left(1 - hx + \frac{h^2}{4} \varepsilon\right) \left(x + \frac{h \varepsilon}{2}\right)}{1 - hx + \frac{h^2}{4} \varepsilon} = x + \frac{h \varepsilon}{2},$$

which shows the existence of  $\gamma_{x(0)}$  (3.31).

We compute the Jacobian matrix associated with (3.29) as

$$\frac{\partial(\tilde{x}, \tilde{y})}{\partial(x, y)} = \begin{pmatrix} \frac{1 - h^2 y - \frac{h^4 \varepsilon^2}{16}}{\left(1 - hx + \frac{h^2 \varepsilon}{4}\right)^2} & -\frac{h}{1 - hx + \frac{h^2 \varepsilon}{4}} \\ \frac{h \varepsilon - h^2 \varepsilon x + \frac{h^3 \varepsilon}{4} (2x^2 - 2y + \varepsilon) - \frac{h^4 \varepsilon^2}{4} x}{\left(1 - hx + \frac{h^2 \varepsilon}{4}\right)^2} & \frac{1 - hx - \frac{h^2 \varepsilon}{4}}{1 - hx + \frac{h^2 \varepsilon}{4}} \end{pmatrix}. \quad (3.35)$$

In particular, observe that for  $(x, y) \in S$  we have

$$\frac{\partial \tilde{x}}{\partial x}(x, y) = \frac{-h^2 x^2 + \left(1 + \frac{h^2 \varepsilon}{4}\right)^2}{\left(1 - hx + \frac{h^2 \varepsilon}{4}\right)^2} =: J_h(x). \quad (3.36)$$

Clearly,  $J_h(0) = 1$ . Moreover, we observe for all  $x \in \mathbb{R} \setminus \left\{\left(1 + \frac{h^2 \varepsilon}{4}\right) / h\right\}$  that

$$J'_h(x) = \frac{2h\left(1 + \frac{h^2 \varepsilon}{4}\right)}{\left(1 - hx + \frac{h^2 \varepsilon}{4}\right)^2} > 0.$$

This concludes the claim.  $\square$

Similarly to the transcritical and the pitchfork case, let  $\rho \in O(1)$  be a positive constant and set  $x(0) = -\rho$ . Similar to what we have done for the other singularities, we are going to consider the variational equation along  $\gamma_{h,-\rho}$  only in the  $x$ -direction. Note that the only point along  $\gamma_{h,-\rho}$  that is tangent to a horizontal line is at  $p_0 = (x, y) = \left(0, -\frac{\varepsilon}{2} - \frac{\varepsilon^2 h^2}{8}\right)$ . However, it follows from (3.35) that  $\frac{\partial \bar{x}}{\partial x}(p_0) = 1$ , meaning that at  $p_0$  there is no contraction nor expansion. This observation indeed allows us to only focus on the factors  $\frac{\partial \bar{x}}{\partial x}(x, y)$  as contraction/expansion rates giving

$$v_1(n) = \prod_{k=0}^n J_h \left( -\rho + \frac{\varepsilon h k}{2} \right) \quad \forall n \geq 0.$$

When  $\rho = \varepsilon h N / 2$  for some  $N \in \mathbb{N}$ , then  $\gamma_{h,-\rho} = \gamma$ , i.e. we are on the special canard (3.34). As before, we introduce

$$\begin{aligned} v^*(m) &:= \prod_{k=0}^m J_h \left( \frac{\varepsilon h k}{2} \right) \quad \forall m \geq 0, \\ v^*(m) &:= \prod_{k=m}^0 J_h \left( \frac{\varepsilon h k}{2} \right) \quad \forall m \leq 0, \end{aligned} \tag{3.37}$$

and observe that for all  $n \geq N$

$$v_1(n) = v^*(-N)v^*(n-N). \tag{3.38}$$

This leads to the following statement, analogously to Proposition 3.2 and Proposition 3.5:

**Proposition 3.7.** *For any  $h, \varepsilon > 0$  such that  $\frac{2}{\varepsilon h^2} + \frac{1}{2} \notin \mathbb{N}$ , consider the entry point  $x(0) = -\rho < 0$ .*

1. *If  $\rho = \varepsilon h N / 2$  for some  $N \in \mathbb{N}$ , then the way-in/way-out map  $\psi_h$  given by*

$$\begin{aligned} 1 &= \prod_{k=0}^{N+\psi_h(-N)} \left| J_h \left( -\rho + \frac{\varepsilon h k}{2} \right) \right| = |v_1(N + \psi_h(-N))| \\ &= |v^*(-N)v^*(\psi_h(-N))|, \end{aligned}$$

*is well defined and takes the value*

$$\psi_h(-N) = N.$$

*In other words, the accumulated contraction and expansion rates compensate each other in perfect symmetry.*

2. *If, generally,  $\rho \in (\varepsilon h N / 2, \varepsilon h (N + 1) / 2)$  for some  $N \in \mathbb{N}$  such that  $\left(1 + \frac{h^2 \varepsilon}{4}\right) / h \neq \gamma_{-\rho}^1(n)$  for all  $n \in \mathbb{N}$ , then the way-in/way-out map  $\psi_h(-N)$  is given by the smallest natural number such that*

$$1 \leq \prod_{k=0}^{N+\psi_h(-N)} \left| J_h \left( -\rho + \frac{\varepsilon h k}{2} \right) \right| = |v_1(N + \psi_h(-N))|,$$

*and satisfies*

$$\psi_h(-N) \in \{N + 1, N + 2\}. \tag{3.39}$$

Summarising both cases, we conclude that the expansion has compensated for contraction at

$$x^* \in \{\rho - \varepsilon h, \rho, \rho + \varepsilon h\},$$

giving full symmetry of the entry-exit relation.

*Proof.* We show that  $J_h(x)J_h(-x) = 1$  for all  $x \neq (1 + h^2/4)/h$ . Then the first claim follows immediately.

$$\begin{aligned} J_h(x)J_h(-x) &= \\ &= \frac{-h^2x^2 + \left(1 + \frac{h^2}{4}\right)^2}{h^2x^2 - 2\left(xh + \frac{h^3}{4}x\right) + \left(1 + \frac{h^2}{4}\right)^2} \frac{-h^2x^2 + \left(1 + \frac{h^2}{4}\right)^2}{h^2x^2 + 2\left(xh + x\frac{h^3}{4}\right) + \left(1 + \frac{h^2}{4}\right)^2} \\ &= \frac{h^4x^4 - 2\left(hx + \frac{h^3}{4}x\right)^2 + \left(1 + \frac{h^2}{4}\right)^4}{h^4x^4 - 4\left(hx + \frac{h^3}{4}x\right)^2 + 2\left(hx + \frac{h^3}{4}x\right)^2 + \left(1 + \frac{h^2}{4}\right)^4} = 1. \end{aligned}$$

The second claim can be deduced from arguments analogously to the proof of Proposition 3.2 and Proposition 3.4.  $\square$

**Remark 3.8.** *Again, contraction and expansion balance out completely along the canard solution for the Kahan map which mirrors exactly the time-continuous case where*

$$v^*(\rho) = \int_0^\rho 2x \, dx,$$

such that the way-in/way-out map  $\psi$  satisfies  $\psi(\rho) = -\rho$  for all  $\rho \in I \subset \mathbb{R}$  for some appropriate interval  $I$ . We can make the starting and end point of the time-continuous and time-discrete system coincide exactly when simply choosing  $\rho = \frac{\varepsilon hn}{2}$  for some  $n \in \mathbb{N}$ .

## 4 Numerical simulations

In Figure 3 we showcase the analysis we have performed in Sections 2 and 3 by numerical simulations. The following remarks supplement our illustrations:

**Remark 4.1.**

- *We only present simulations for  $\varepsilon = 1$  since for  $\varepsilon \ll 1$ , some numerical issues appear, which we do not aim to resolve within this paper: most importantly, the exponential contraction towards the canard is much stronger for  $\varepsilon \ll 1$  than for the choice  $\varepsilon = 1$ . Thus, depending on the initial conditions and on the numerical precision of the implementation, the distance between a trajectory and the canard may become “numerically zero”.*
- *Related to the previous point, we recall that the orbits of a fast-slow system  $X(x, \varepsilon)$  are equivalent to the orbits of  $X(x, 1)$  for  $\varepsilon > 0$  even around singularities of the critical manifold. This can be shown, for example, using the blow-up method [18]. This is why, the delay effect that one observes for  $\varepsilon = 1$  is still present for  $\varepsilon \ll 1$ ; it is just harder to be observed numerically.*

- We present simulations only for the transcritical singularity as it allows us to compare the RK and the Kahan schemes. Recall that for the pitchfork singularity the Kahan scheme is not explicit, while for the fold singularity, the forward-Euler discretisation (and by that the most basic explicit RK-discretisation) does not provide a canard.
- Recall from Proposition 2.9 that, in order to observe the extended delay of the bifurcation, a critical triplet  $(\rho^*, h^*, \varepsilon^*)$ , given as a solution of  $1 + hQ_s(-\rho) = 0$ , must exist. Since  $Q_s$  is an  $s$ -degree polynomial, the existence of such a critical triplet is guaranteed for  $s$  being odd, while for  $s$  being even, one needs to carefully choose the scheme and the parameters  $(h, \varepsilon)$ . Therefore, we have used a 3-stage RK method for the simulation depicted in Figure 3.

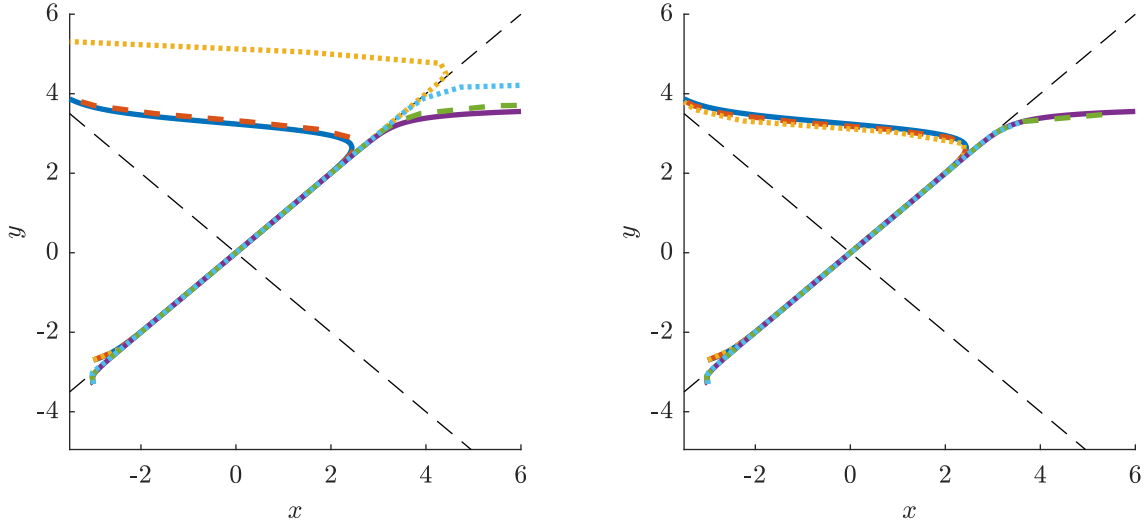


Figure 3: Comparison of a simulation of a fast-slow system with a transcritical singularity. The simulation on the left corresponds to a 3-stage RK scheme, while the one on the right corresponds to the Kahan scheme. These simulations have the same initial conditions  $(x, y) = \{(-\rho, -0.9\rho), (-\rho, -1.1\rho)\}$  with  $\rho = 3$  and the three types of trajectories correspond to the values of  $h = (1 \times 10^{-4}, 0.2, 0.2865)$  shown as solid, dashed and dotted curves respectively. For the choice of  $\rho = 3$  the critical value  $h^*$  is  $h^* \approx 0.28$ . Thus, the diagram on the left shows that when  $h$  is close to the critical  $h^*$  one observes an extended delay on the loss of stability of the canard. We emphasize that such a delay can be made arbitrarily long by appropriately choosing  $h^*$ . Compare to the right panel, where the extended delay does not occur upon variation of  $h$ .

## 5 Conclusion

We have shown that explicit Runge-Kutta schemes can fail to provide accurate approximations of dynamical behaviour along canard trajectories for certain combinations of step size  $h$  and entry coordinates  $(x_0, y_0)$  in the plane. In fact, RK-schemes are prone to show much longer delays on the onset of bifurcation than that one expects from the continuous time cases. It is worth noting that for maps, such an extra delay is not a phenomenon due to time scale separation, but a truly discretisation artefact. We have quantified such phenomenon for simple canonical forms of planar

fast-slow problems: hence, we emphasize that, also for more complicated systems, one should be cautious when simulating trajectories close to canards and trying to find entry-exit relations.

Additionally, we have proven that an implicit Runge-Kutta scheme like the Kahan method, which gives an explicit birational map for quadratic vector fields, preserves the symmetry of the linearisation around planar canards. One might ask whether other structure-preserving schemes such as symplectic methods could also provide such symmetries. However, in the pitchfork and transcritical case, there is no conserved quantity, and in the case of the folded canard the conserved quantity is not a Hamiltonian which makes the usage of symplectic methods cumbersome (see also [12]). We leave it as an open question to investigate a more general categorization of time discretisation schemes which preserve symmetries of the linearisation along canards to give accurate approximations of the dynamics.

## Acknowledgements

The authors gratefully acknowledge C. Kuehn for pointing out the Jensen inequality. ME is supported by the SFB grant “discretisation in Geometry and Dynamics” sponsored by the German Research Foundation (DFG). HJK is supported by the Alexander von Humboldt Foundation.

## References

- [1] L. Arcidiacono, M. Engel, and C. Kuehn. Discretized fast-slow systems near pitchfork singularities. *J. Difference Equ. Appl.*, 25(7):1024–1051, 2019.
- [2] E. Benoît, J. Callot, F. Diener, and M. Diener. Chasse au canards. *Collect. Math.*, 31:37–119, 1981.
- [3] R. Bertram and J. E. Rubin. Multi-timescale systems and fast-slow analysis. *Mathematical biosciences*, 287:105–121, 2017.
- [4] H. Boudjellaba and T. Sari. Dynamic transcritical bifurcations in a class of slow–fast predator–prey models. *Journal of Differential Equations*, 246(6):2205–2225, 2009.
- [5] E. Celledoni, R. I. McLachlan, B. Owren, and G. R. W. Quispel. Geometric properties of Kahan’s method. *J. Phys. A*, 46(2):025201, 12, 2013.
- [6] J. H. Conway and R. Guy. *The book of numbers*. Springer Science & Business Media, 2012.
- [7] P. De Maesschalck and M. Wechselberger. Neural excitability and singular bifurcations. *The Journal of Mathematical Neuroscience (JMN)*, 5(1):16, 2015.
- [8] M. Desroches, J. Guckenheimer, B. Krauskopf, C. Kuehn, H. M. Osinga, and M. Wechselberger. Mixed-mode oscillations with multiple time scales. *Siam Review*, 54(2):211–288, 2012.
- [9] *NIST Digital Library of Mathematical Functions*. <http://dlmf.nist.gov/>, Release 1.0.24 of 2019-09-15. F. W. J. Olver, A. B. Olde Daalhuis, D. W. Lozier, B. I. Schneider, R. F. Boisvert, C. W. Clark, B. R. Miller, B. V. Saunders, H. S. Cohl, and M. A. McClain, eds.
- [10] F. Dumortier and R. Roussarie. Canard cycles and center manifolds. *Mem. Amer. Math. Soc.*, 121(577):x+100, 1996. With an appendix by Cheng Zhi Li.

- [11] M. Engel and C. Kuehn. Discretized fast-slow systems near transcritical singularities. *Nonlinearity*, 32(7):2365–2391, 2019.
- [12] M. Engel, C. Kuehn, M. Petrera, and Y. Suris. Discretized fast-slow systems with canard points in two dimensions. *arXiv:1907.06574*, 2019.
- [13] N. Fenichel. Geometric singular perturbation theory for ordinary differential equations. *J. Differential Equations*, 31:53–98, 1979.
- [14] R. Gray, A. Franci, V. Srivastava, and N. E. Leonard. Multiagent decision-making dynamics inspired by honeybees. *IEEE Transactions on Control of Network Systems*, 5(2):793–806, 2018.
- [15] M. G. Hayes, T. J. Kaper, P. Szmolyan, and M. Wechselberger. Geometric desingularization of degenerate singularities in the presence of fast rotation: A new proof of known results for slow passage through hopf bifurcations. *Indagationes Mathematicae*, 27(5):1184–1203, 2016.
- [16] M. W. Hirsch, C. C. Pugh, and M. Shub. *Invariant manifolds*. Lecture Notes in Mathematics, Vol. 583. Springer-Verlag, Berlin-New York, 1977.
- [17] H. Jardón-Kojakhmetov and C. Kuehn. On fast-slow consensus networks with a dynamic weight. *arXiv preprint arXiv:1904.02690*, 2019.
- [18] H. Jardón-Kojakhmetov and C. Kuehn. A survey on the blow-up method for fast-slow systems. *arXiv preprint arXiv:1901.01402*, 2019.
- [19] C. K. R. T. Jones. Geometric singular perturbation theory. In *Dynamical systems (Montecatini Terme, 1994)*, volume 1609 of *Lecture Notes in Math.*, pages 44–118. Springer, Berlin, 1995.
- [20] W. Kahan. *Unconventional numerical methods for trajectory calculations*. Unpublished lecture notes, 1993.
- [21] M. Krupa and P. Szmolyan. Relaxation oscillation and canard explosion. *J. Differential Equations*, 174(2):312–368, 2001.
- [22] C. Kuehn. *Multiple time scale dynamics*, volume 191 of *Applied Mathematical Sciences*. Springer, Cham, 2015.
- [23] J. Mitry, M. McCarthy, N. Kopell, and M. Wechselberger. Excitable neurons, firing threshold manifolds and canards. *The Journal of Mathematical Neuroscience*, 3(1):12, 2013.
- [24] A. Neishtadt. Persistence of stability loss for dynamical bifurcations i. *Differential Equations*, 23:1385–1391, 1987.
- [25] A. Neishtadt. Persistence of stability loss for dynamical bifurcations ii. *Differential Equations*, 24:171–176, 1988.
- [26] A. Neishtadt. On stability loss delay for dynamical bifurcations. *Discrete & Continuous Dynamical Systems-S*, 2(4):897–909, 2009.
- [27] M. Petrera and Y. Suris. New results on integrability of the kahan-hirota-kimura discretizations. *arXiv:1805.12490*, 2018.

- [28] K. Tsaneva-Atanasova, C. L. Zimlik, R. Bertram, and A. Sherman. Diffusion of calcium and metabolites in pancreatic islets: killing oscillations with a pitchfork. *Biophysical journal*, 90(10):3434–3446, 2006.
- [29] S. Wiggins. *Normally hyperbolic invariant manifolds in dynamical systems*, volume 105 of *Applied Mathematical Sciences*. Springer-Verlag, New York, 1994. With the assistance of György Haller and Igor Mezić.